

# Low threshold monocrySTALLINE Nd:(Gd, Lu)<sub>2</sub>O<sub>3</sub> channel waveguide laser

Andreas Kahn,<sup>1</sup> Sebastian Heinrich,<sup>1</sup> Henning Kühn,<sup>1</sup> Klaus Petermann,<sup>1</sup> Jonathan D. B. Bradley,<sup>2</sup> Kerstin Wörhoff,<sup>2</sup> Markus Pollnau,<sup>2</sup> and Günter Huber<sup>1</sup>

<sup>1</sup>Universität Hamburg, Institut für Laser-Physik, Luruper Chaussee 149, 22761 Hamburg, Germany <sup>2</sup>Integrated Optical MicroSystems (IOMS) Group, MESA+ Institute for Nanotechnology, University of Twente, P.O. Box 217, 7500 AE Enschede, The Netherlands  
[akahn@physnet.uni-hamburg.de](mailto:akahn@physnet.uni-hamburg.de)

**Abstract:** We report the first waveguide laser based on a rare-earth-doped sesquioxide. A 2 μm thick lattice matched Nd(0.5%):(Gd, Lu)<sub>2</sub>O<sub>3</sub> film with a nearly atomically flat surface has been epitaxially grown on a Y<sub>2</sub>O<sub>3</sub> substrate, using pulsed laser deposition. The film has been structured with reactive ion etching and a rib channel waveguide laser has been realized. Laser radiation at 1075 nm and 1079 nm has been observed under 820-nm pumping. The laser possesses a threshold power of about 0.8 mW and a preliminary slope efficiency of 0.5% versus incident pump power. A maximum output power of 1.8 mW has been obtained for 370 mW incident pump power.

© 2009 Optical Society of America

**OCIS codes:** (130.3120) Integrated optics devices; (140.3530) Lasers, neodymium; (140.5680) Rare earth and transition metal solid-state lasers; (230.7380) Waveguides, channeled.

---

## References and links

1. J. I. Mackenzie, "Dielectric Solid-State Planar Waveguide Lasers: A Review," *IEEE J. Select. Topics Quantum Electron.* **13**, 626-637 (2007).
2. R. Peters, C. Kränkel, K. Petermann, and G. Huber, "Broadly tunable high-power Yb:Lu<sub>2</sub>O<sub>3</sub> thin disk laser with 80% slope efficiency," *Opt. Express* **15**, 7075-7082 (2007).
3. C. Grivas and R. W. Eason, "Dielectric binary oxide films as waveguide laser media: a review," *J. Phys.: Condens. Matter* **20**, 264011 (2008).
4. M. Pollnau, C. Grivas, L. Laversenne, J. S. Wilkinson, R. W. Eason, and D. P. Shepherd, "Ti:Sapphire waveguide lasers," *Laser Phys. Lett.* **4**, 560-571 (2007).
5. K. L. Saenger, "Pulsed Laser Deposition (Part I) - A Review of Process Characteristics and Capabilities," *Processing of Advanced Materials* **2**, 1-24 (1993).
6. K. L. Saenger, "Pulsed Laser Deposition (Part II) - A Review of Process Mechanisms," *Processing of Advanced Materials* **3**, 63-82 (1993).
7. G. J. H. M. Rijnders, G. Koster, D. H. A. Blank, and H. Rogalla, "In situ monitoring during pulsed laser deposition of complex oxides using reflection high energy electron diffraction under high oxygen pressure," *Appl. Phys. Lett.* **70**, 1888-1890 (1997).
8. D. S. Gill, A. A. Anderson, R. W. Eason, T. J. Warburton, and D. P. Shepherd, "Laser operation of an Nd:Gd<sub>3</sub>Ga<sub>5</sub>O<sub>12</sub> thin-film optical waveguide fabricated by pulsed laser deposition," *Appl. Phys. Lett.* **69**, 10-12 (1996).
9. T. Gün, A. Kahn, B. İleri, K. Petermann, and G. Huber, "Two-dimensional growth of lattice matched Nd-doped (Gd,Lu)<sub>2</sub>O<sub>3</sub>-films on Y<sub>2</sub>O<sub>3</sub> by pulsed laser deposition," *Appl. Phys. Lett.* **93**, 053108 (2008).
10. A. Kahn, H. Kühn, S. Heinrich, K. Petermann, J. D. B. Bradley, K. Wörhoff, M. Pollnau, Y. Kuzminykh, and G. Huber, "Amplification in epitaxially grown Er:(Gd, Lu)<sub>2</sub>O<sub>3</sub> waveguides for active integrated optical devices," *J. Opt. Soc. Am. B* **25**, 1850-1853 (2008).

11. E. Lallier, J. P. Pocholle, M. Papuchon, C. Grezes-Besset, E. Pelletier, M. De Micheli, M. J. Li, Q. He, and D. B. Ostrowsky, "Laser oscillation of single-mode channel waveguide in Nd: MgO:LiNbO<sub>3</sub>," *Electron. Lett.* **25**, 1491-1492 (1989).
12. S. J. Field, D. C. Hanna, A. C. Large, D. P. Shepherd, A. C. Tropper, P. J. Chandler, P. D. Townsend, and L. Zhang, "Ion-implanted Nd:GGG channel waveguide laser," *Opt. Lett.* **17**, 52-54 (1992).
13. R. Gerhardt, J. Kleine-Börger, L. Beilschmidt, M. Frommeyer, H. Dötsch, and B. Gather, "Efficient channel-waveguide laser in Nd:GGG at 1.062 μm wavelength," *Appl. Phys. Lett.* **75**, 1210-1212 (1999).
14. A. G. Okhrimchuk, A. V. Shestakov, I. Khrushchev, and J. Mitchell, "Depressed cladding, buried waveguide laser formed in a YAG:Nd<sup>3+</sup> crystal by femtosecond laser writing," *Opt. Lett.* **30**, 2248-2250 (2005).
15. J. D. B. Bradley, F. Ay, K. Wörhoff, and M. Pollnau, "Fabrication of low-loss channel waveguides in Al<sub>2</sub>O<sub>3</sub> and Y<sub>2</sub>O<sub>3</sub> layers by inductively coupled plasma reactive ion etching," *Appl. Phys. B* **89**, 311-318 (2007).
16. K. Wörhoff, J. D. B. Bradley, F. Ay, D. Geskus, T. P. Blauwendraat, and M. Pollnau, "Reliable low-cost fabrication of low-loss Al<sub>2</sub>O<sub>3</sub>:Er<sup>3+</sup> waveguides with 5.4-dB optical gain," *IEEE J. Sel. Top. Quantum Electron.* Accepted for publication (2008).
17. H. Kühn, S. T. Fredrich-Thornton, C. Kränkel, R. Peters, and K. Petermann, "Model for the calculation of radiation trapping and description of the pinhole method," *Opt. Lett.* **32**, 1908-1910 (2007).
18. L. Fornasiero, "Nd<sup>3+</sup> and Tm<sup>3+</sup>-dotierte Sesquioxide," Ph.D. thesis, Universität Hamburg (1999).
19. H. P. Weber, P. F. Liao, and B. C. Tofield, "Emission cross section and fluorescence efficiency of Nd-pentaphosphate," *IEEE J. Quantum Electron.* **10**, 563-567 (1974).

## 1. Introduction

Due to the light confinement in optical waveguides, which results in an excellent mode overlap of pump and laser light, waveguide lasers generally exhibit high optical gain and a low threshold. This is already true for planar waveguide lasers [1], but particularly in channel waveguides, which provide a two-dimensional light confinement. Such waveguide lasers are very promising, as they offer a high potential for miniaturization and can lead to more complex integrated optical devices, featuring multiple active and passive elements on a small chip.

Crystalline rare-earth (RE) doped dielectric oxides are well suited for the realization of lasers with high frequency stability or high (peak) power, since they possess sharp emission peaks and high peak cross sections. Especially the sesquioxides have been proven to be very attractive host materials for RE based lasers [2], as they feature relatively low phonon energies, high thermal conductivities and damage thresholds. While several groups are involved in the research of RE-doped sesquioxide films [3], lasing in such waveguides has not yet been reported. In fact, waveguide lasers based on dielectric binary oxide films have so far only been demonstrated with Ti:Al<sub>2</sub>O<sub>3</sub> [4] and Nd:Ta<sub>2</sub>O<sub>5</sub> [3]. In this paper we report the first RE-doped sesquioxide waveguide laser.

A flexible method for the fabrication of thin films is pulsed laser deposition (PLD) [5, 6, 7]. The first planar waveguide laser based on PLD films has been realized by Gill et al. [8]. Recently, it has been shown that epitaxial growth of lattice matched RE:(Gd, Lu)<sub>2</sub>O<sub>3</sub> on Y<sub>2</sub>O<sub>3</sub> with PLD is possible [9], resulting in monocrystalline films with nearly atomically flat surfaces. The spectroscopic properties of such films have been investigated in [10], showing fluorescence lifetimes and emission cross sections similar to correspondingly doped Y<sub>2</sub>O<sub>3</sub> bulk crystals. Due to the excellent laser properties of the neodymium ion, Nd<sup>3+</sup> doped (Gd, Lu)<sub>2</sub>O<sub>3</sub> films were chosen for the demonstration of a first RE-doped sesquioxide waveguide laser. For instance, several other Nd<sup>3+</sup> doped oxides have already been proven to be suitable for the realization of channel waveguide lasers [11, 12, 13, 14].

## 2. Waveguide preparation

In addition to the 1 μm thick (Nd<sub>0.005</sub>, Gd<sub>0.479</sub>, Lu<sub>0.516</sub>)<sub>2</sub>O<sub>3</sub> film presented in [9], a 2 μm thick (Nd<sub>0.005</sub>, Gd<sub>0.487</sub>, Lu<sub>0.508</sub>)<sub>2</sub>O<sub>3</sub> film was produced by PLD with similar deposition parameters. The beam of a KrF excimer laser at 248 nm with a pulse width of 20 ns was focused onto a sintered ceramic target, resulting in a laser fluence of about 1.5 – 2 J/cm<sup>2</sup>. Both films were

grown on {100} oriented, epitaxial grade polished  $\text{Y}_2\text{O}_3$  substrates (10 mm  $\times$  10 mm  $\times$  0.5 mm), which were positioned at a distance of 9.5 cm from the target and heated to 900 °C. The deposition took place in an  $\text{O}_2$ -atmosphere of  $9 \times 10^{-3}$  mbar. Epitaxial film growth was proven *in situ* by reflection high energy electron diffraction monitoring and atomically smooth terraces as well as atomic steps have been identified by atomic force microscopy. The 2  $\mu\text{m}$  thick planar waveguide was structured by reactive ion etching, as described in [15], resulting in straight rib channel waveguides with widths ranging from about 2 to 5  $\mu\text{m}$  and an etch depth of 300 nm. These channel dimensions were chosen to support one transverse mode at 1079 nm only. The film was then covered by sputtering a 1.8  $\mu\text{m}$  thick amorphous  $\text{Al}_2\text{O}_3$  layer, as described in [16], in order to reduce scattering at the surface as well as prevent damage and edge rounding of the waveguiding layer during the following polishing of the end facets. Polishing of the structured sample resulted in a waveguide length of 6 mm.

### 3. Spectroscopic characterization

Lifetime measurements and optical spectroscopy were performed on the unstructured sample at room temperature. The  $\text{Nd}^{3+}$  ion density of the 0.5at.% doped film is expected to be  $1.34 \times 10^{20}$   $\text{cm}^{-3}$ , as for 0.5at.% doped  $\text{Y}_2\text{O}_3$ , which possesses a nearly identical crystal structure and lattice constant. A fluorescence lifetime  $\tau = 258$   $\mu\text{s}$  of the  ${}^4\text{F}_{3/2}$  ( $\text{Nd}^{3+}$ ) multiplet was determined from the luminescence decay curves of the  ${}^4\text{F}_{3/2} \rightarrow {}^4\text{I}_{11/2}$  transition upon pulsed excitation at 820 nm. The measurement was performed for different excitation volumes, realized by using differently sized pinholes [17]. Since the results only vary by about 5%, radiation trapping seems to have no significant effect on the measured lifetime. The lifetime of the lattice matched  $\text{Nd}(0.5\%):(\text{Gd}, \text{Lu})_2\text{O}_3$  film is comparable with the lifetimes of 275  $\mu\text{s}$  and 238  $\mu\text{s}$ , which were measured in [18] for a  $\text{Nd}(0.3\%):\text{Y}_2\text{O}_3$  and a  $\text{Nd}(1.1\%):\text{Y}_2\text{O}_3$  bulk crystal, respectively. Therefore, the radiative lifetime  $\tau_{\text{rad}} = 410$   $\mu\text{s}$ , which was derived in [18] from the spectroscopic data of the above mentioned  $\text{Nd}:\text{Y}_2\text{O}_3$  bulk crystals, was assumed to be valid as well for the lattice matched film.

The emission cross sections of the  ${}^4\text{F}_{3/2} \rightarrow {}^4\text{I}_{11/2}$  transitions were determined from the fluorescence spectrum of the  $\text{Nd}:(\text{Gd}, \text{Lu})_2\text{O}_3$  film by use of the Füchtbauer-Ladenburg equation [19]. Therein, a branching ratio  $\beta = 47$  % was assumed, as determined for  $\text{Nd}:\text{Y}_2\text{O}_3$  in [18]. Figure 1 shows the emission cross section spectrum, measured with a spectral bandwidth of 0.32 nm, in comparison with the one measured in [18] for a  $\text{Nd}(1.1\%):\text{Y}_2\text{O}_3$  bulk crystal.

The peak positions of emission in the  $\text{Nd}:(\text{Gd}, \text{Lu})_2\text{O}_3$  film are nearly the same as those measured for the  $\text{Nd}:\text{Y}_2\text{O}_3$  bulk crystal. This can be explained by the epitaxial growth and nearly perfect lattice matching. However, a spectral broadening of the emission peaks in the film, resulting in lower peak cross sections, can be observed. This is probably due to the statistical occupation of the cation sites by  $\text{Gd}^{3+}$  and  $\text{Lu}^{3+}$ .

### 4. Waveguide properties

The Cauchy parameters measured for an  $(\text{Er}_{0.006}, \text{Gd}_{0.494}, \text{Lu}_{0.500})_2\text{O}_3$  film reported in [10] were applied as well to the  $\text{Nd}:(\text{Gd}, \text{Lu})_2\text{O}_3$  films, resulting in refractive indexes of 1.93 and 1.92 for wavelengths around 800 nm and 1080 nm, respectively. Since the RE doping is very small and the  $\text{Gd}_2\text{O}_3$  and  $\text{Lu}_2\text{O}_3$  content is quite similar, the refractive indexes of these  $\text{Er}^{3+}$  and  $\text{Nd}^{3+}$  doped films are most likely comparable. The positive refractive index difference of 0.03 between film and substrate results in a numerical aperture (NA) of 0.34. To estimate the propagation losses in the structured sample, laser light from a  $\text{Ti}:\text{Al}_2\text{O}_3$  laser at 780 nm was coupled into a waveguide channel by use of a microscope objective with a NA of 0.35. The outcoupled light was collected by a microscope objective with a NA of 0.7 and the outcoupled laser power  $P_{\text{out}}$  compared with the power  $P_{\text{in}}$ , measured before coupling into the waveguide.

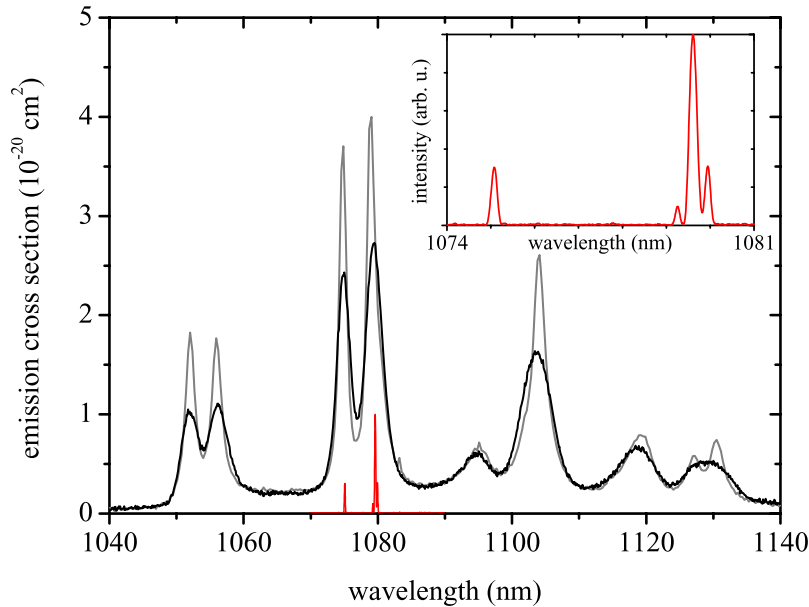


Fig. 1. Emission cross sections of a Nd:(Gd, Lu)<sub>2</sub>O<sub>3</sub> film (black curve) in comparison with the ones measured in [18] for a Nd:Y<sub>2</sub>O<sub>3</sub> bulk crystal (grey curve). The waveguide laser spectrum (intensity in arbitrary units) is plotted as red curve and magnified in the inset.

Taking the Fresnel reflections at the end facets and the transmission of the outcoupling objective into account, an upper limit of the waveguide losses  $L = 4.8$  dB at 780 nm was determined with

$$L = -10 \times \log \frac{P_{\text{out}}}{P_{\text{in}}} \text{dB}. \quad (1)$$

Since the absorption cross section is very low at 780 nm, absorption losses can be neglected. However, additional coupling losses, such as those resulting from an imperfect overlap between the pump and waveguide mode, are still included in  $L$ . The propagation losses for the 6 mm long waveguide channel are thus lower than 4.8 dB. The losses are most likely due to scattering at imperfections smaller than the wavelength and at particulates in the micrometer range, which are produced during the ablation process. Probably the propagation losses are lower at longer wavelengths, due to a smaller impact of Rayleigh scattering.

## 5. Laser experiments

The polished end facets of the structured waveguide were directly coated with reflective mirrors. While a highly reflective (HR) coating for 1000 – 1100 nm was applied on the incoupling facet, about 1 – 2% transmission for this wavelength range was realized at the outcoupling side. A Ti:Al<sub>2</sub>O<sub>3</sub> laser beam at 820 nm was used for excitation. It was coupled into a waveguide channel, as displayed in Fig. 2. The same objectives as described in section 4 were used for the coupling. Additionally, two dichroic mirrors, which were HR for the pump light, served as filters. Since these filters weren't aligned to couple light back into the waveguide and the

reflectivity for the pump light at the outcoupling side was only about 16%, the pumping scheme is single pass.

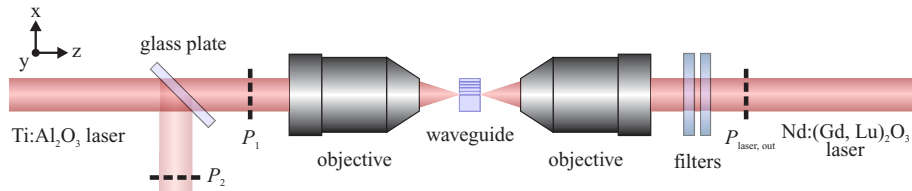


Fig. 2. Waveguide laser setup. A Ti:Al<sub>2</sub>O<sub>3</sub> laser beam at 820 nm was coupled into a waveguide channel, using a microscope objective with a NA of 0.35. The outcoupled light was collected by a microscope objective with a NA of 0.7. Two dichroic mirrors were used as filters for the pump light. A thin glass plate served as beam splitter to measure input and output power simultaneously.  $P_1$ ,  $P_2$  and  $P_{\text{laser,out}}$  indicate positions used for these power measurements.

Laser action with a heavily damped relaxation oscillation of about 300  $\mu\text{s}$  was demonstrated. The relaxation oscillation was visualized on an oscilloscope by chopping the pump beam and measuring the intensity variations of the outcoupled light at 1079 nm with a silicon photodiode behind a monochromator. Lasing occurred on four wavelengths at about 1075 nm and 1079 nm simultaneously, as seen in Fig. 1. The spectrum was measured using a Fourier spectrometer with 0.1 nm resolution. Figure 3 shows the transverse intensity profile of the outcoupled laser light, which was recorded with a CCD camera.

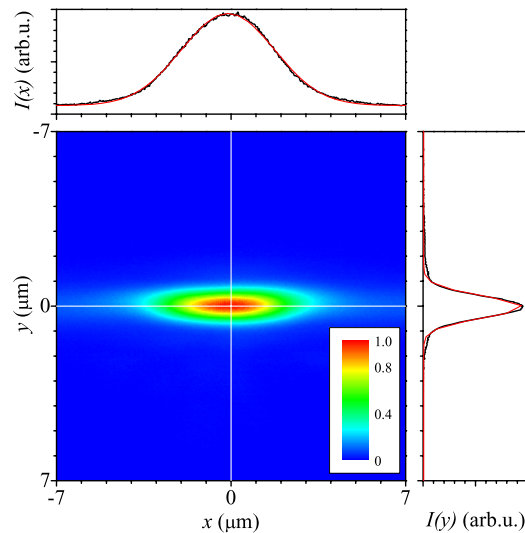


Fig. 3. Intensity distribution of the outcoupled laser light. The corresponding intensity profiles  $I(x)$  and  $I(y)$  (black curves) are fitted with Gaussian functions (red curves).

The output power  $P_{\text{laser,out}}$  of the waveguide laser for various pump powers  $P_{\text{pump,in}}$  is plotted in Fig. 4. The input power was varied slowly while  $P_{\text{pump,in}}$  and  $P_{\text{laser,out}}$  were recorded simultaneously. A thin glass plate served as beam splitter and the pump power  $P_2$  reflected from the

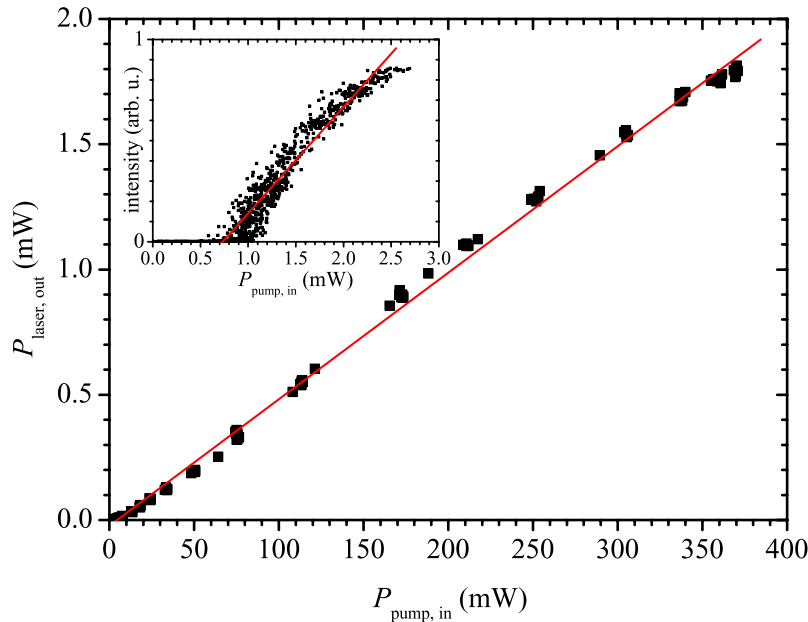


Fig. 4. Laser output power  $P_{\text{laser,out}}$  plotted against the incident pump power  $P_{\text{pump,in}}$ . A slope efficiency of 0.5 % has been determined with a linear fit (red curve) of the measured data points (black squares). The inset shows the measurement results (black squares) for the determination of the laser threshold with a linear fit (red curve).

glass plate was measured simultaneously with  $P_{\text{laser,out}}$ . A calibration measurement was performed to derive the power  $P_1$  which was transmitted through the glass plate from the reflected power  $P_2$ .  $P_{\text{pump,in}}$  was determined from  $P_1$  by taking the transmission of the incoupling objective as well as the reflectivity of the incoupling mirror at the pump wavelength into account. Additional coupling losses were not considered. The power of pump light coupled into the waveguide channel is therefore smaller than  $P_{\text{pump,in}}$ .  $P_{\text{laser,out}}$  was corrected by considering the transmission of the outcoupling objective and dichroic mirrors.

A maximum output power of  $P_{\text{laser,out}} = 1.8$  mW was obtained for  $P_{\text{pump,in}} = 370$  mW incident pump power. The absorbed pump power could not be determined, due to the unknown coupling efficiency and high waveguide losses. A slope efficiency of 0.5 % with respect to the incident pump power was calculated from the input-output curve in Fig. 4. The slope efficiency with respect to the absorbed pump power is most likely significantly higher. Due to light confinement in the extremely small waveguide dimensions, the laser threshold is very small and could not be determined reliably from the input-output curve. Thus, instead of measuring  $P_{\text{laser,out}}$ , the signal of a silicon photodiode behind a monochromator was measured in dependence of  $P_{\text{pump,in}}$  (see inset of Fig. 4). For increased accuracy, the pump beam was chopped and the lock-in technique applied. The bend in the measured data points can most likely be explained by a saturation of the photodiode. Therefore, the data points for pump powers above 2 mW were ignored and a laser threshold of approximately 0.8 mW was determined.

## 6. Conclusions

The first waveguide laser based on the promising RE-doped sesquioxides has been realized. Using PLD, a monocrystalline Nd<sup>3+</sup> doped (Gd, Lu)<sub>2</sub>O<sub>3</sub> film was epitaxially grown on Y<sub>2</sub>O<sub>3</sub>. Structuring the film by reactive ion etching and coating the end-facets, a rib channel waveguide laser has been realized. Due to the light confinement in the small waveguide dimensions, the laser possesses a very low threshold power of approximately 0.8 mW. A slope efficiency of 0.5% versus incident pump power and a maximum output power of 1.8 mW have been demonstrated. Higher output powers and slope efficiencies can be realized by increasing the output coupling above 2%. Furthermore, the laser performance can most likely be significantly increased by reducing the waveguide losses. Most probably, particulates in the micrometer range, which are generated during the ablation process, contribute highly to these losses. Therefore, by implementing a particle filter into the PLD setup, waveguides with significantly lower losses could be produced. However, the material system supports a waveguide laser even with the high losses probably introduced by the deposition technique. Therefore, the investigated material system is a very promising candidate for the realization of more complex integrated optical devices, like ring lasers with a high frequency stability. This could lead to the implementation of multiple active and passive integrated optical devices on a small chip.

## Acknowledgments

We acknowledge the support of the European Commission within the specific targeted research project PI-OXIDE (017 501). Furthermore, we would like to thank Dieter Barlösius for applying the reflective coatings on the waveguide end-facets and Meidert Dijkstra for performing the reactive ion etching.